Studies in Conservation

Material characterisation for preserving cultural heritage: Evidence of the 1595 fire at Pisa Cathedral

--Manuscript Draft--

Manuscript Number:	SIC1592R1
Full Title:	Material characterisation for preserving cultural heritage: Evidence of the 1595 fire at Pisa Cathedral
Article Type:	Original Research or Treatment Paper
Keywords:	Stone masonry; fire; damage; Pb; calcarenite
Corresponding Author:	Simona Raneri ICCOM CNR Pisa: Istituto di Chimica dei Composti Organo Metallici Consiglio Nazionale delle Ricerche Sezione di Pisa ITALY
Corresponding Author Secondary Information:	
Corresponding Author's Institution:	ICCOM CNR Pisa: Istituto di Chimica dei Composti Organo Metallici Consiglio Nazionale delle Ricerche Sezione di Pisa
Corresponding Author's Secondary Institution:	
First Author:	Simona Raneri
First Author Secondary Information:	
Order of Authors:	Simona Raneri
	Dario Pancani
	Anna De Falco
	Nadia Montevecchi
	Anna Gioncada
Order of Authors Secondary Information:	
Abstract:	Recent restoration work on Pisa Cathedral provided the opportunity for a multidisciplinary analysis of the monument that identified interesting aspects of its history, conservation and structural safety. In particular, the study of the matroneum provided clues about the role of the structures in the well-known fire that occurred in 1595. Alteration patterns and damage forms on the stone masonry walls were analysed to better understand their relationship with this catastrophic event. The investigation of the stone specimens enabled textural and mineralogical features typical of fire damage to be identified on the surface. The evidence of fire also provided a terminus ante quem to correctly interpret and diachronically date a damage pattern consisting of cracks in the eastern arch supporting the dome. The cracks were likely to have been induced by a soil consolidation phenomenon related to the renowned leaning of the Pisa tower, centuries before the fire.
Funding Information:	

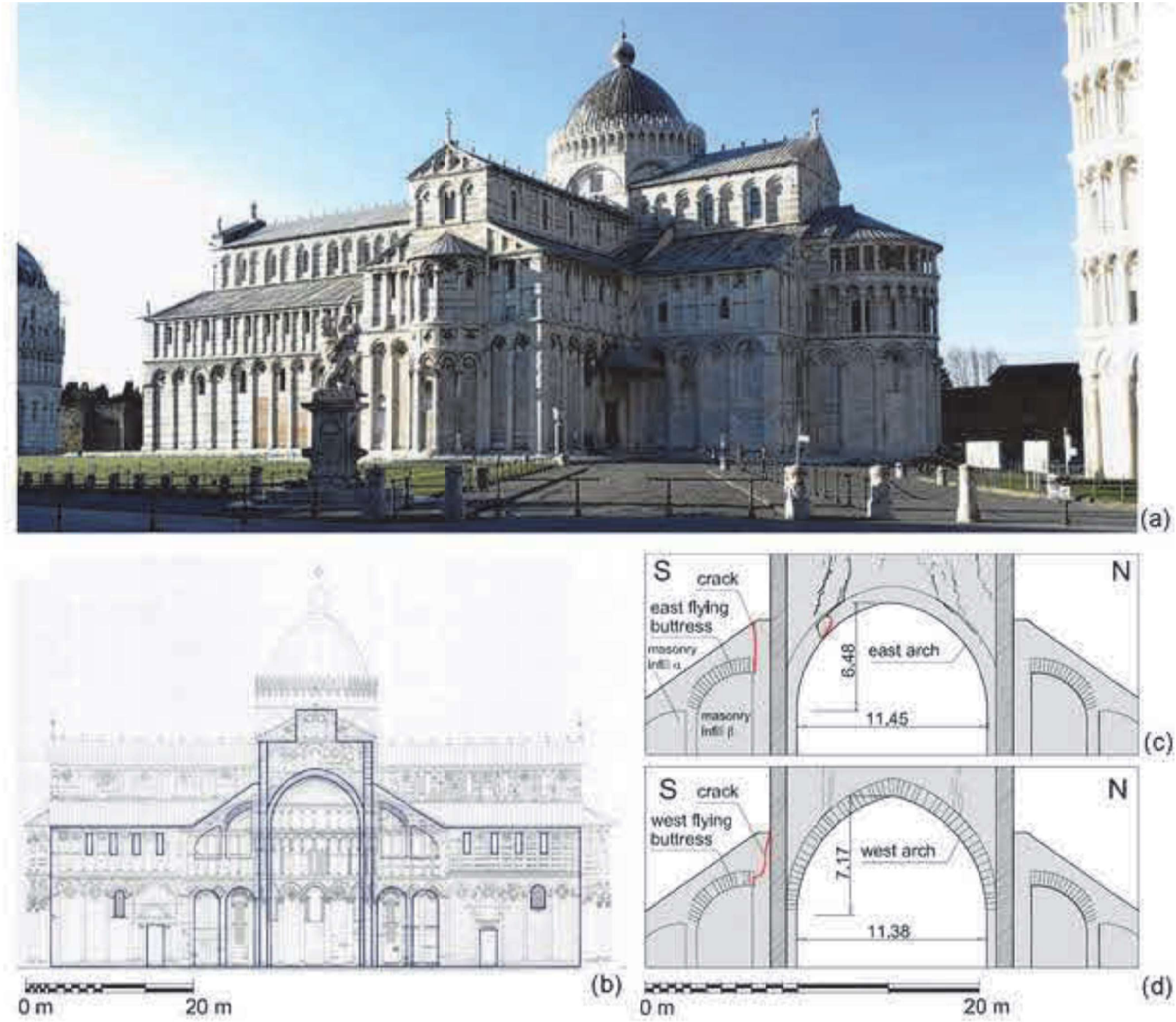

Figure 2

Click here to access/download;Colour figure;Figure2.jpg

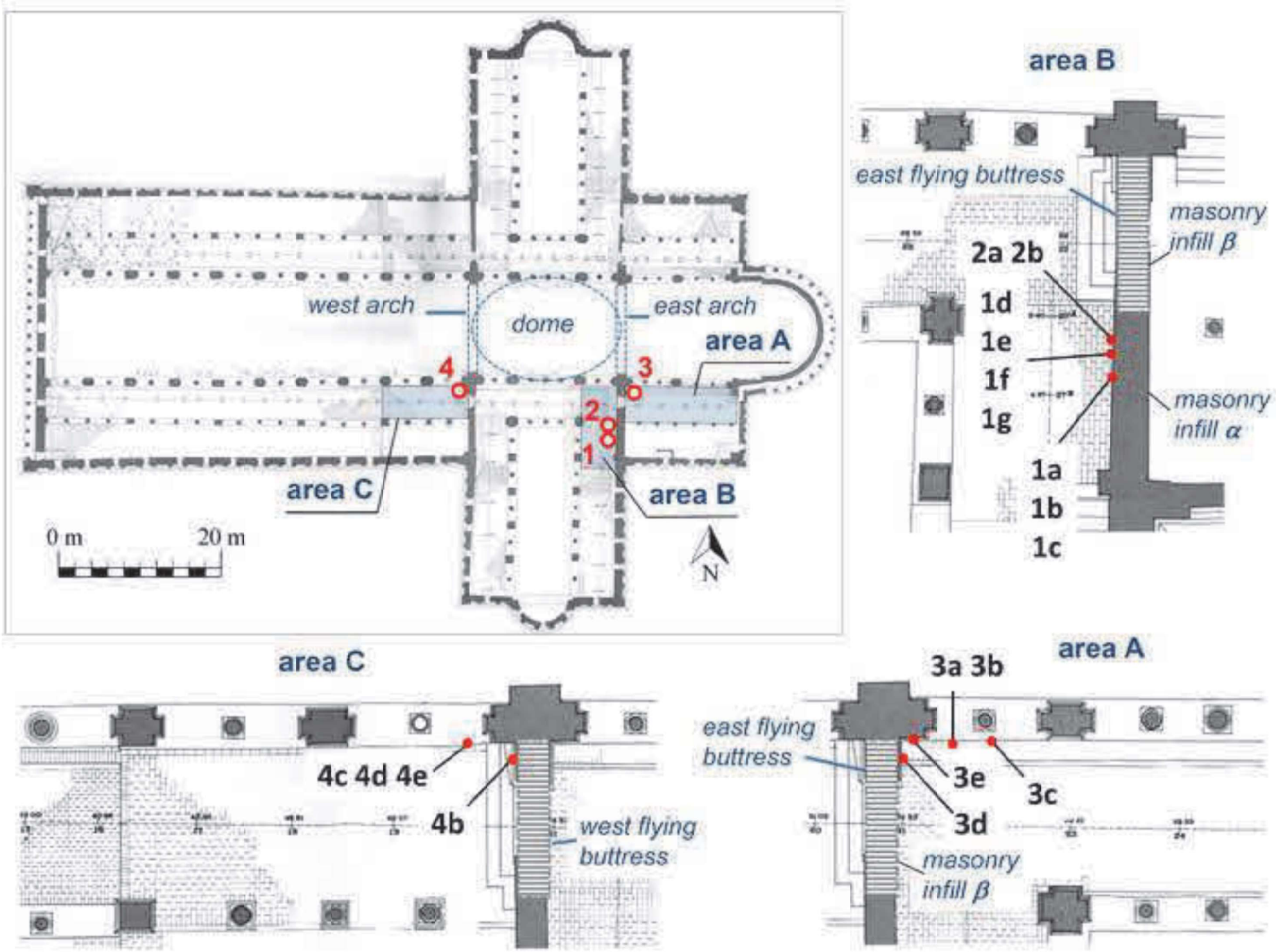

Figure 3

Click here to access/download;Colour figure;Figure3.jpg

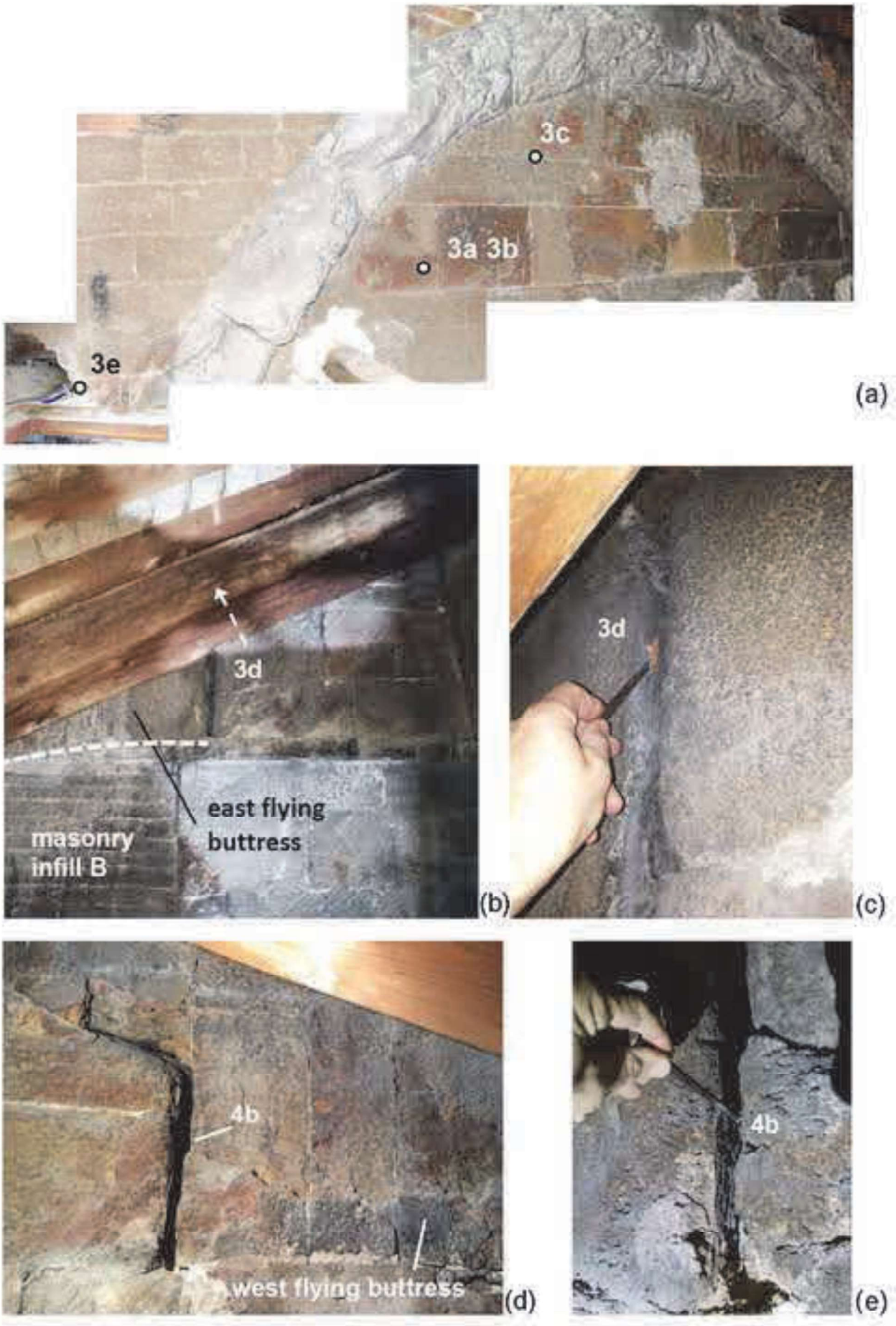

Figure 4

Click here to access/download;Colour figure;Figure4.jpg

Figure 5

Click here to access/download;Colour figure;Figure5.jpg

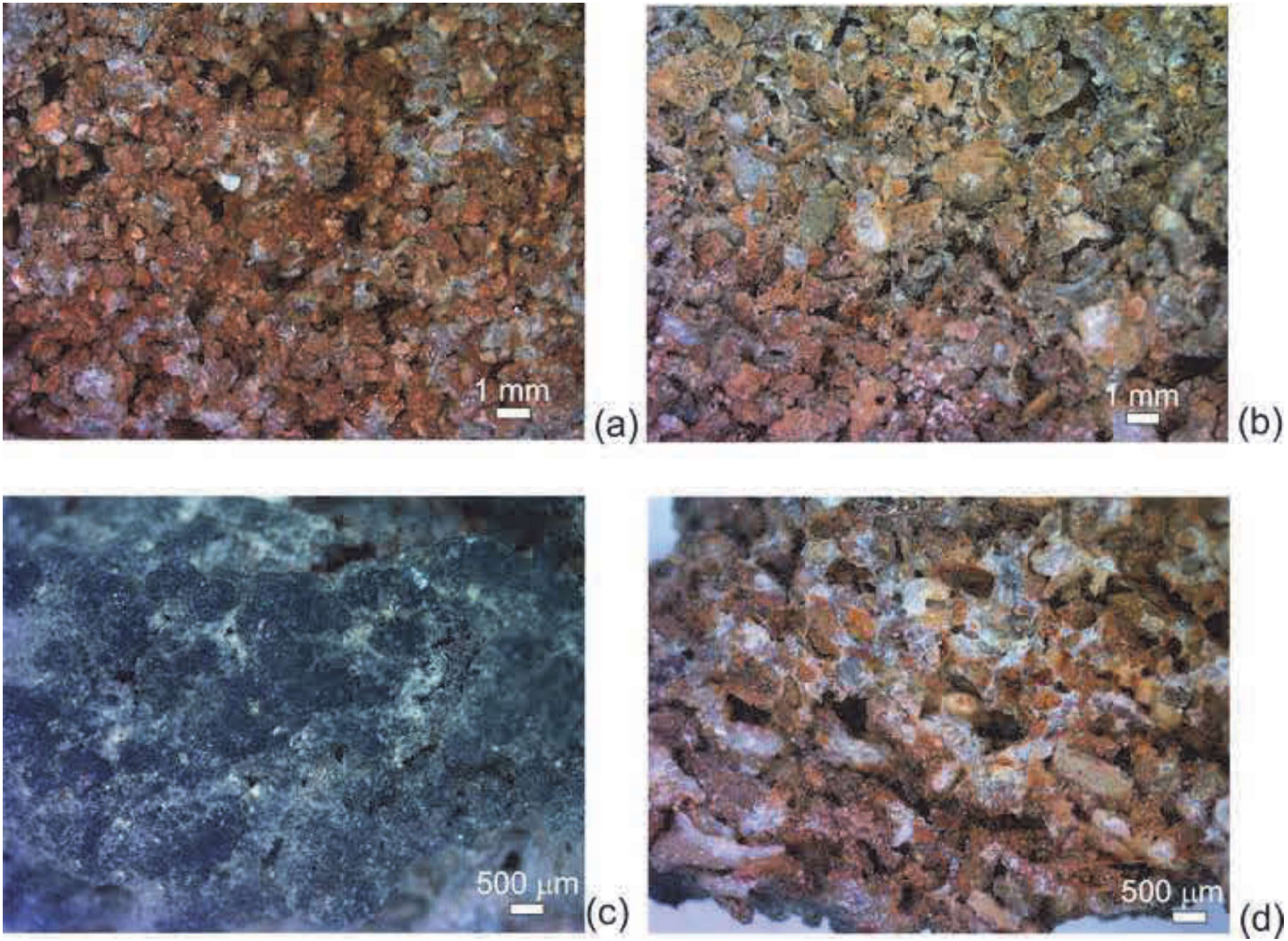

Figure 6

Click here to access/download;Colour figure;Figure6.jpg

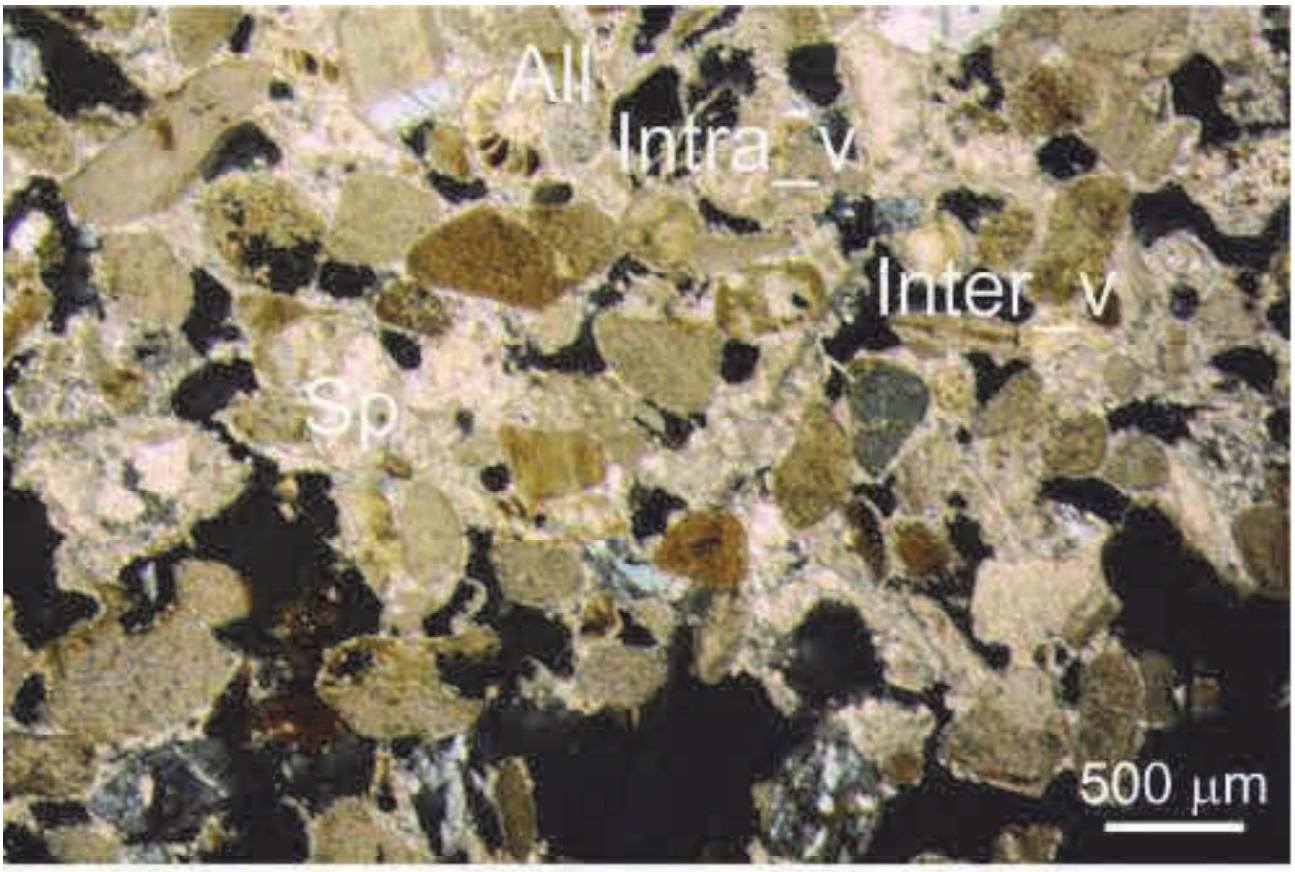

(a)

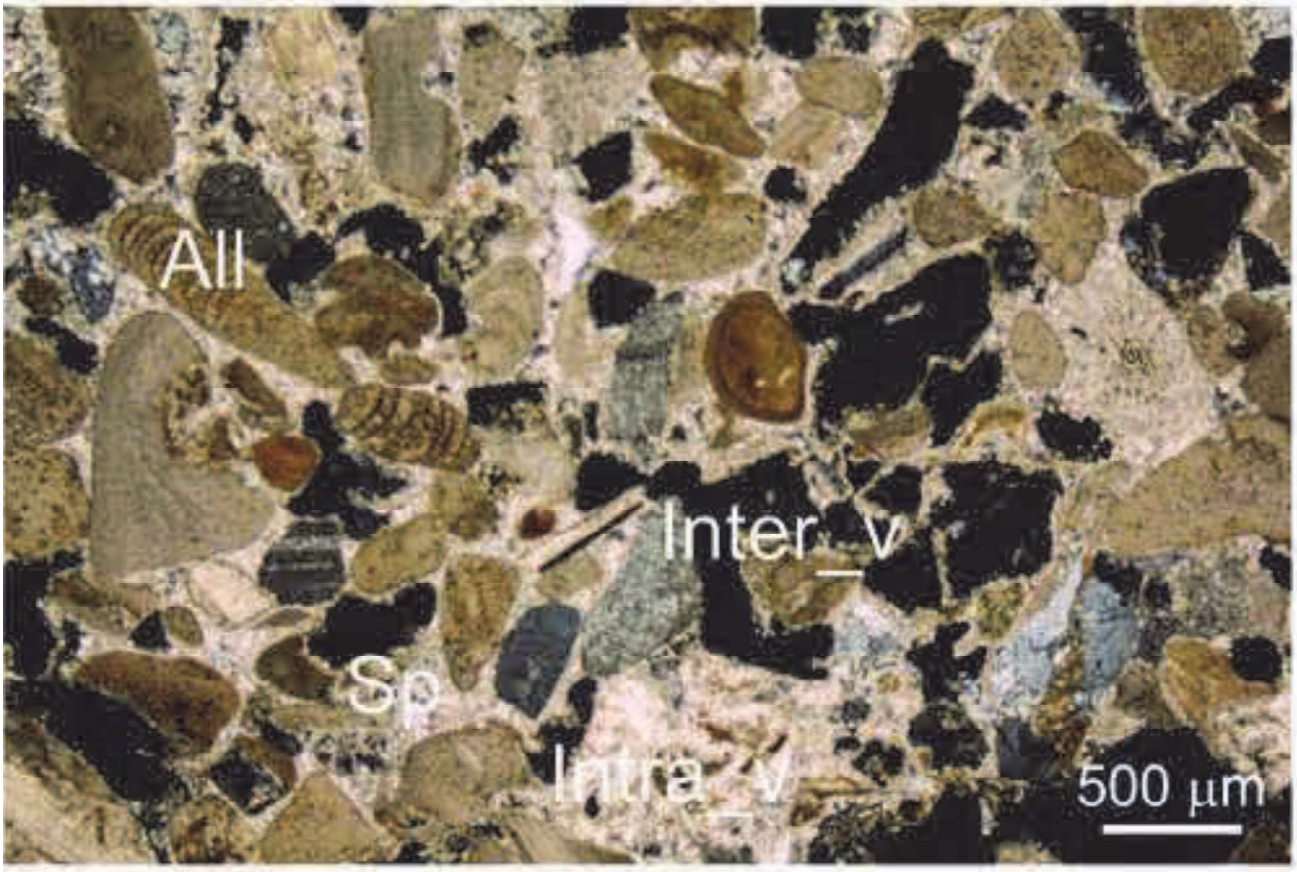

(b)

Figure 7

Click here to access/download;Colour figure;Figure7.jpg

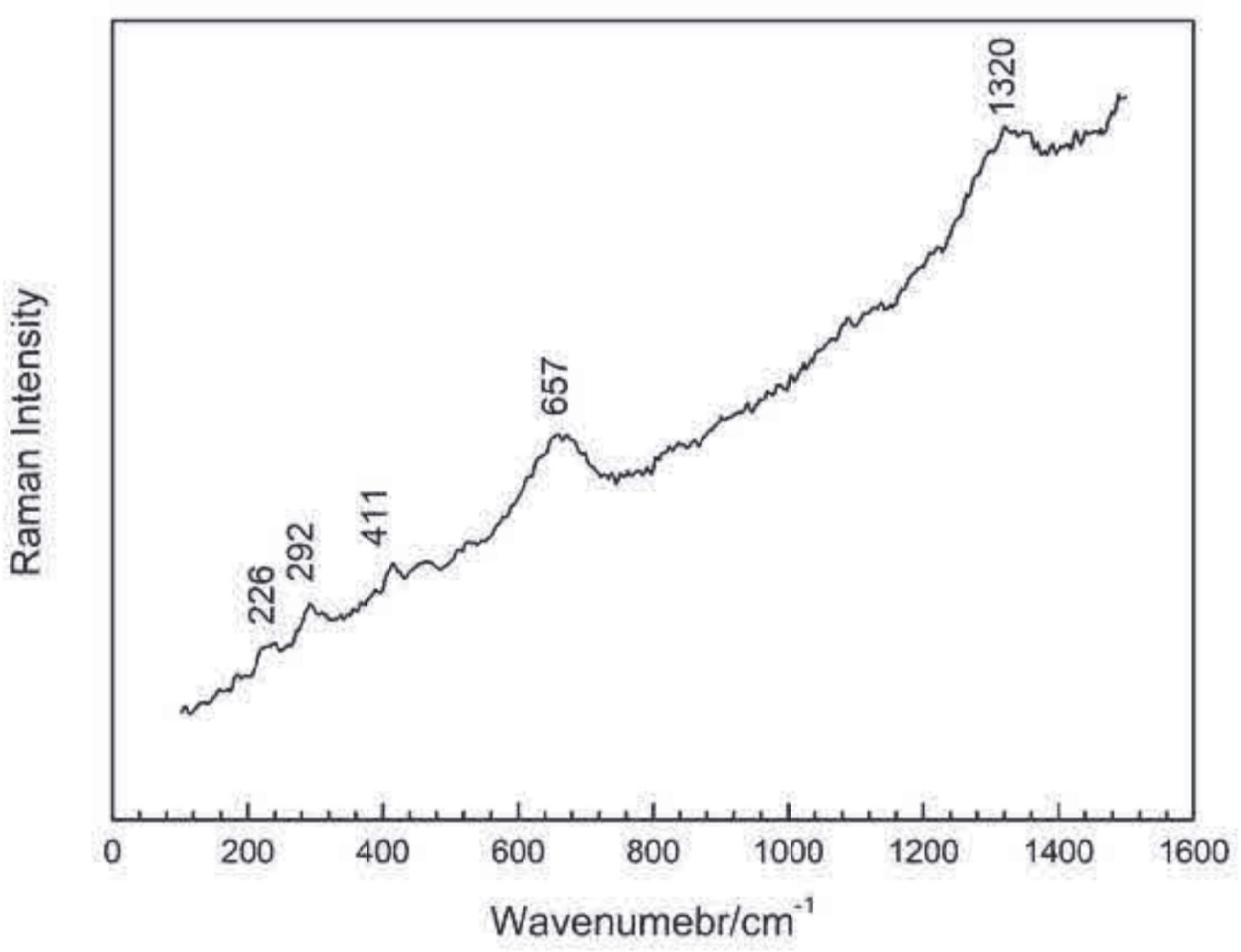

Figure 8

Click here to access/download;Colour figure;Figure8.jpg

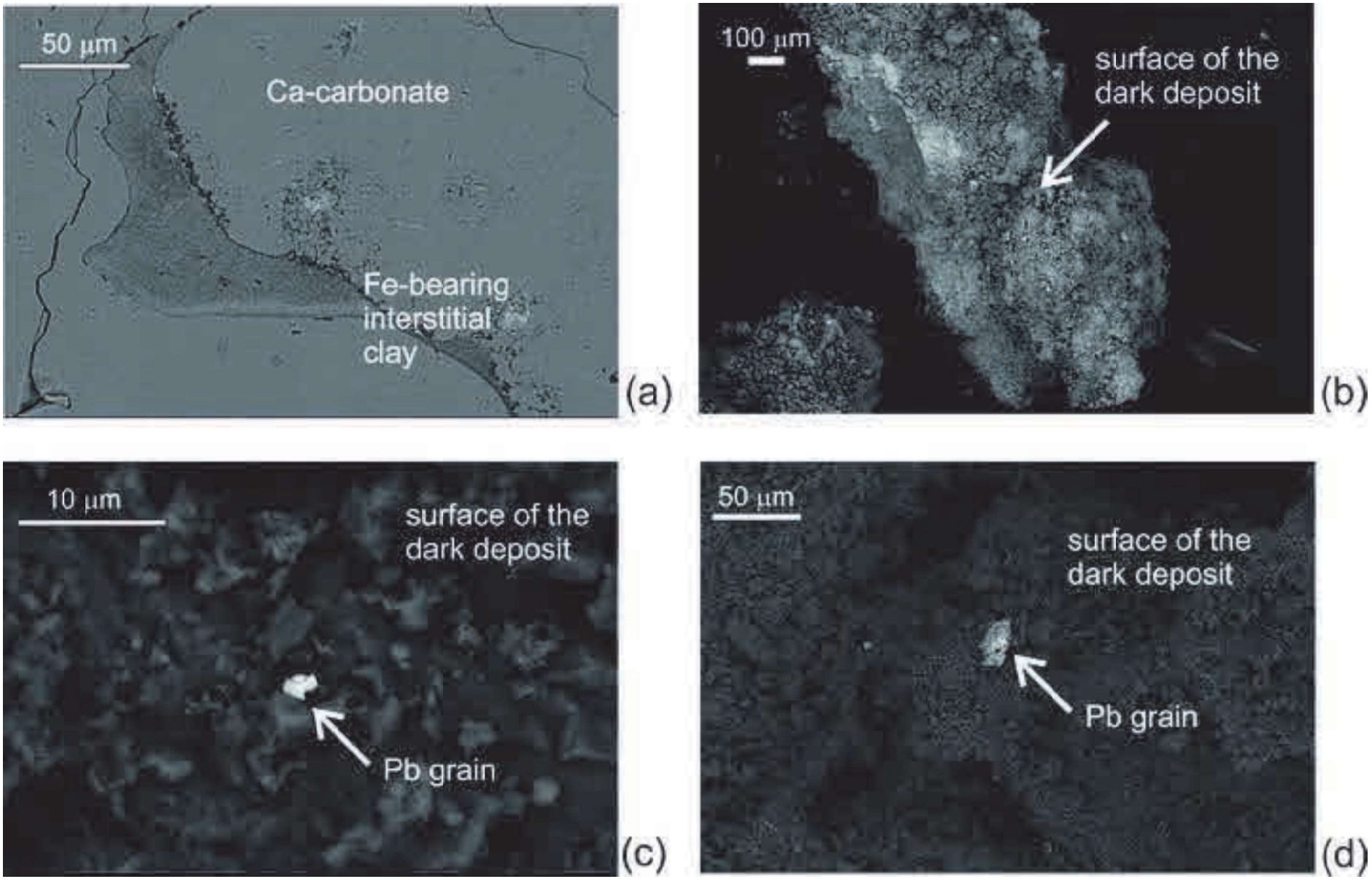

Figure 9

Click here to access/download;Colour figure;Figure9.jpg

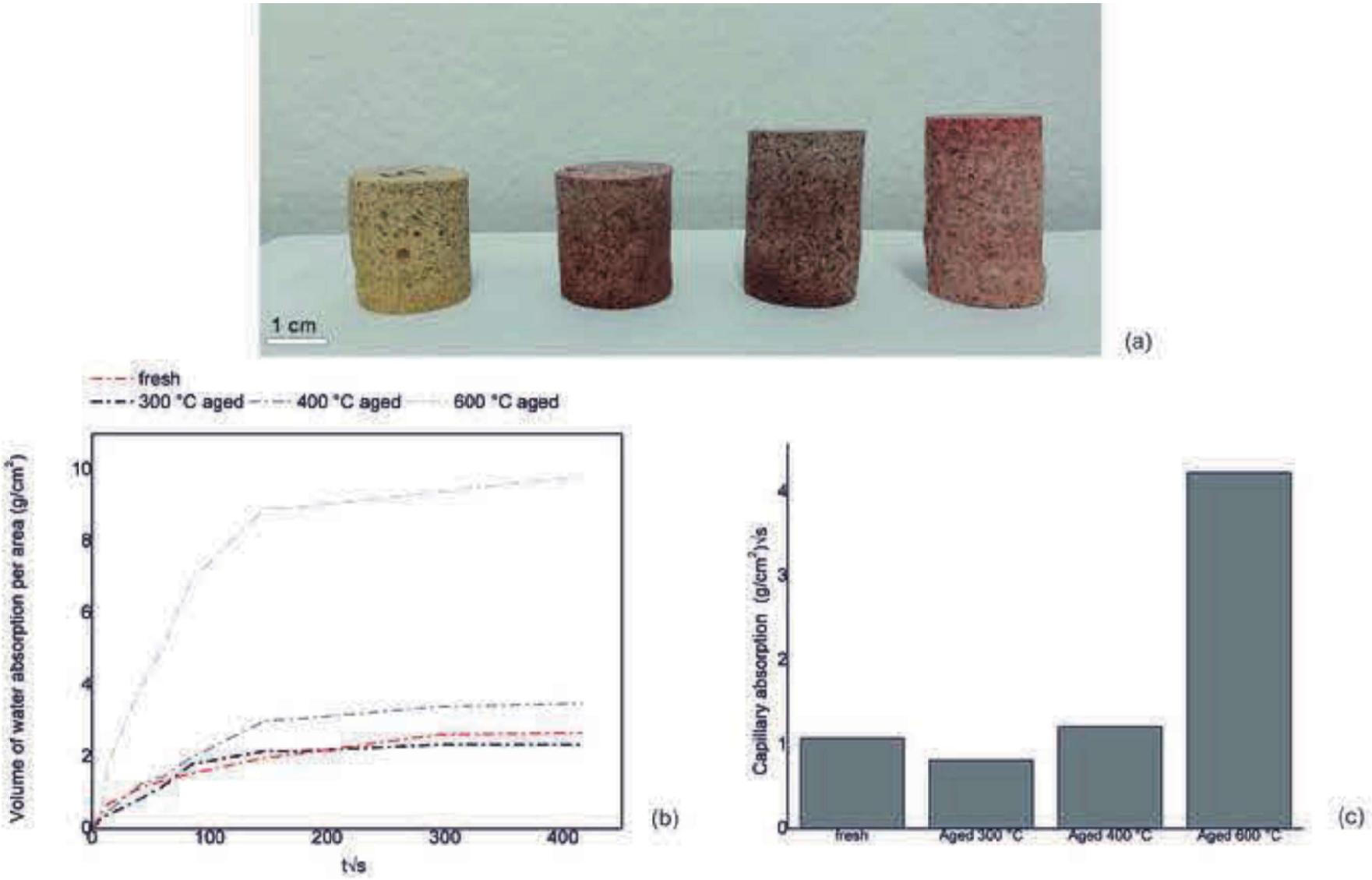

Figure 10

Click here to access/download;Colour figure;Figure10.jpg

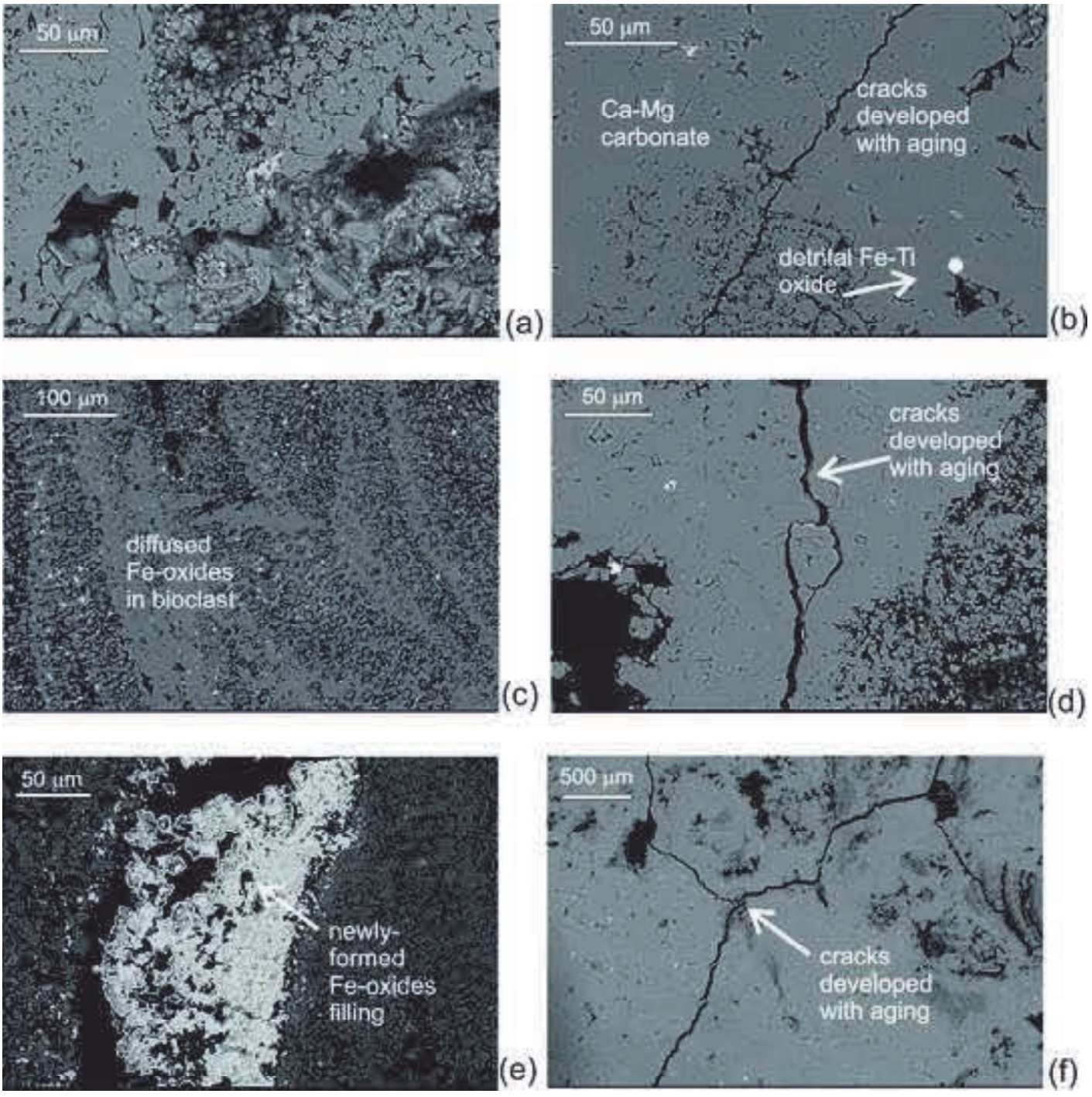

Material characterisation for preserving cultural heritage: Evidence of the 1595 fire at Pisa Cathedral

S. Raneri[1,2,*], D. Pancani[1], A. De Falco[3], N. Montevecchi[4], A. Gioncada[1]

[1]University of Pisa, Department of Earth Sciences, Via Santa Maria, 53, 56126, Pisa, Italy

[2]National Research Council, ICCOM-CNR, Via G. Moruzzi 1, 56124 Pisa, Italy

[3] University of Pisa, Department of Civil and Industrial Engineering (DICI), Largo Lucio Lazzarino, 1, 56122, Pisa, Italy

[4]Dedalo s.a.s. Diagnosi e Conoscenza Storica del Patrimonio Culturale – via Pontormo, 49, 59016 Poggio a Caiano - Prato

corresponding author: simona.raneri@pi.iccom.cnr.it

Abstract

Recent restoration work on Pisa Cathedral provided the opportunity for a multidisciplinary analysis of the monument that identified interesting aspects of its history, conservation and structural safety. In particular, the study of the *matroneum* provided clues about the role of the structures in the well-known fire that occurred in 1595. Alteration patterns and damage forms on the stone masonry walls were analysed to better understand their relationship with this catastrophic event. The investigation of the stone specimens enabled textural and mineralogical features typical of fire damage to be identified on the surface. The evidence of fire also provided a *terminus ante quem* to correctly interpret and diachronically date a damage pattern consisting of cracks in the eastern arch supporting the dome. The cracks were likely to have been induced by a soil consolidation phenomenon related to the renowned leaning of the Pisa tower, centuries before the fire.

Keywords

Stone masonry, fire, damage, Pb, calcarenite.

Introduction

The effects of global changes on monuments have been extensively evaluated in recent years, mainly to ensure their protection from natural and anthropogenic hazards. Fires represent extremely dangerous natural hazards for heritage structures. They can cause irreversible damage to construction materials, compromising the cohesion of the architectural stone elements.

The high temperatures produced by fires can induce severe physico-mechanical and compositional changes in the natural stones and artificial geomaterials that constitute the buildings. Different architectural elements can be differently affected by fire. The visible effects are function of the intensity, the maximum temperatures at the surface and the duration of exposure to the fire, while thermal stresses occur with specific material properties (McCabe et al. 2007a, b, 2010; Brotons et al. 2013; Andriani and Germinario 2014). An adequate analysis of the effects of fire on architectural elements usually requires a multi-methodological approach, particularly with natural stones, as damage to them is due to the interplay of physical and mineralogical changes.

More than 50 papers have been published on this topic over the past 30 years (Martinho and Dionisio 2020), and provide evidence of the advantages and limitations of different methodological approaches in evaluating fire

damage and structural resilience to natural hazards. Fires cause identifiable patterns of alteration and degradation, whose effects are particularly evident in specific stone substrates. These patterns have been classified by ISCS (2008) into fractures and deformation, material loss, detachments, and colour change due to material loss or the presence of deposits. One of the most visible effects of fires is the development of fractures, whose geometry and distribution increase the stone's susceptibility to further decay (Yavuz et al. 2010). The damage consists of fissures or detachment (at the millimetre to centimetre scale), or inter/intracrystal fractures at a microscale, the latter ones due to mineralogical reactions or phase transitions (Jansen et al. 1993). Recent studies of the effect of fires on carbonate stones have demonstrated that at temperatures higher than 600 °C calcite and dolomite start to dissociate and CO_2 is released, which is responsible for microfractures and volume changes (Kilic and Anil 2006; Galai et al. 2007; Sippel et al. 2007), and thus damaged stones are more susceptible to external agents (Gunasekaran and Anbalagan 2007). In terms of chromatic alteration, colour changes are typically due to mineralogical transformations at high temperature. Regardless of the stone type, colour change appears negligible between 150 °C and 200 °C (Beck et al. 2016; Vazquez et al 2016), whereas at higher temperatures up to 400 °C stone surfaces are affected by a colour change from yellow to red, and in some cases by blacking (Kompanikova et al. 2014; McCabe et al. 2010; Pires et al. 2014). At above 800 °C, carbonate stones, sandstones and marble whiten (Borg et al. 2013; Ozguven and Ozcelik 2013). Studies carried out on carbonate stones have found that a colour alteration from yellow to red can be due to the dehydration of iron compounds (*e.g.*, goethite turning in hematite) or the formation of iron oxides after clay minerals breakdown (Beck et al. 2016; Hajpal and Torok 2004). In sandstones, colour changes are mainly attributed to the oxidation of iron-bearing minerals, such as glauconite (changing from greenish to brownish), and chlorite (yellowing) (Hajpal 2002; Hajpal and Torok, 2004). Tests carried out on ashlars exposed to fire have found that a sharp zone separates the altered surface (2-3 cm thick) and the unaltered area underneath the stone surface (Hajpal 2002). The combination of mineralogical transformations, fracture development and surface deposits are responsible for significant changes in the physical and mechanical properties of stones, mainly due to their porosity and pore distribution modifications. In general, at between 150 °C and 300 °C the number of interconnected pores is reduced, due to mineral collapse (Yavuz et al. 2010). A temperature increase can also cause the opening of new fracture systems, thus promoting the growth of secondary porosity (Martinho and Dionisio, 2020). A similar trend (*i.e.*, initial decrease and rapid increase) has also been found in terms of the roughness of the stone surface (Gomez-Heras et al., 2008).

In studies of ancient masonry, a complete knowledge of the building materials used is essential for understanding the structural damage and resilience (Woodcock 1997; Watt 1999) and to ensure improved restoration strategies are successfully applied.

Pisa Cathedral is an intriguing case, as the restoration work launched in 2012 brought to light interesting alteration and damage patterns on its architectural masonry, whose features suggest the involvement of the structures in fire. Stone samples were thus obtained from altered and damaged structures and analysed through minero-petrographic, spectroscopic, micro-morphological and chemical methods. These investigations were aimed at defining the alteration and the eventual crack patterns and to understand their relationships and connections to the devastating fire the Cathedral suffered in 1595.

Pisa Cathedral and the 1595 fire

The Santa Maria Assunta Cathedral was founded in 1064 and consecrated on 26 September, 1118. The Cathedral was built under the direction of the architect Buscheto, to whom the original layout is attributed, consisting of the basilica with four aisles and one nave and a transept with two aisles and one nave. Rainaldo later extended the west part of the nave. The building was not completed until the last quarter of the XII century, when Bonanno's bronze leaves were placed on the central door. At the end of the 16th century, a fire devastated the Cathedral (Alberti et al. 2011; Ascani 2014; Casini 1986). Following this event, restoration and refurbishment were necessary: the roof was rebuilt, the three bronze doors of the façade restored, and a major decorative undertaking was started. The walls were gradually covered with paintings and large canvases representing the stories of the blessed and saints from Pisa.

The Cathedral is built from lithotypes commonly used in the historical buildings of the city (Ramacciotti et al. 2015) (Fig. 1.a). Monti Pisani marble mainly covers the external surfaces and a yellowish calcarenite traditionally quarried nearby from south of Livorno (Tuscany) (Panchina Fm.; Franzini 1993) is present both the inside and on the upper structures of the Cathedral, at the walls of the *matroneum*, the drum of the dome and the spandrels. The length of the cathedral is about 94 m in the east-west direction and 70 m in the north-south direction, with a height of about 27 m to the top of the roof and 46 m to the top of the dome. An elliptical dome with a maximum of around 20 m stands out at the intersection of the transept with the central nave, resting on two limestone arches with a clear span of about 11.5 m (Fig. 1.b).

Surveys during the 2012 restoration works

The on-going restoration work began in 2012, and provide the opportunity to examine the *material context* of the building, which represents a previously unexplored historical record (Montevecchi and Sutter 2014), along with features related to its structural stability (Bennati et al. 2020). The petrographic survey carried out in the *matroneum* noted a huge chromatic alteration of the stone surface on a coarse-grained calcarenite, which changed its colour from yellow to deep red; in some areas, dark deposits at the stone surface may be related to the effects of a fire. In terms of structural behaviour, recent investigations revealed a crack pattern on the east arch supporting the dome, which is probably related to the effects of soil consolidation. The cracks were discovered on the south side of the east arch, with the typical characteristics of an excessive compression stress state. By analysing the adjacent structures, more damage was found on the flying buttress adjacent to the east arch, consisting of a separation between the end stone ashlars that continues upward, in the form of cracks on the masonry above (Fig. 1.c). On the ashlar surfaces inside the gap generated by the damage, the stone is affected by extensive chromatic alterations and dark deposits, similar to the other architectural structures at the *matroneum*. The same crack pattern and alterations on the stone surface are also present on the flying buttress adjacent to the west arch supporting the dome, in the south transept (Fig. 1.d). No other similar symptoms were observed in the north transept. An archaeological investigation is also underway on the masonry infill "β" - under the eastern flying buttress (see Fig. 1.c), which is not damaged but is also affected by extensive chromatic alteration. This evidence may help us to date the crack pattern, along with the on-going structural analysis, the archaeological surveys and the petrographic studies.

Materials and Methods

Sampling at Pisa Cathedral

In total, 18 samples of yellow-ochre calcarenite classified as Panchina Fm. calcarenite were carefully removed from the structures of the *matroneum* on the south transept (Fig. 3), where a visual inspection confirmed chromatic alteration due to colour changes (from yellow to red) and dark surface deposits (Table 1). Special attention was also given to damaged structures, by sampling representative altered specimens on the stone surfaces affected by cracks, at the flying buttresses adjacent to both the east and west arches.

Five specimens are from area A (see Fig. 2, inset area A), four of which (labelled as 3.a, 3.b and 3.d) were taken from the internal surface of the wall facing the choir under the blind arcade (Fig.3.a) and one specimen (labelled as 3.d) was taken from the flying buttress adjacent the east arch supporting the dome, corresponding to the crack pattern (Fig.3.b-c).

Nine specimens were sampled from area B (see Fig. 2, inset area B), in the south transept, and most were taken from the stone surface constituting the masonry infill "α", which clearly showed chromatic alteration (labelled as 1.*) (Fig.4). Two specimens (labelled as 2a and 2b) were taken from unaltered masonry. Finally, four specimens (labelled as #4) were taken from area C (see Fig. 2, inset area C); specimens 4c-e were from the inner surface of the wall facing the main nave, and were clearly affected by alteration, while specimen 4b is a chip of the dark deposit entering the crack pattern on the west flying buttress (see Fig. 3.e-d).

Geological samples

Geological samples of Panchina Fm. calcarenite were obtained from around Castiglioncello (Livorno, coordinates 43.401218, 10.404723), close to one of the possible ancient quarries of the lithotype (Sarti et al. 2017). This geological Fm has been extensively used in Tuscany since Etruscan times (Franzini 1993; Galoppini et al. 1996) but the main exploited areas and the ancient quarries are not currently accessible or have been obliterated by recent urbanisation. Five cylinders (2 cm in diameter, 4 cm high) were drilled from the outcropping Fm., avoiding naturally weathered surfaces (Table 1).

Experimental procedures

Specimens taken from Pisa Cathedral were examined under a microscope equipped with a ZEISS Axiocam ERc 5s to identify the structural and textural features, along with the morphological features of altered surface and deposits. A selection of samples representative of the locations and alteration forms were examined in thin section with transmitted light under an optical Zeiss Axioplan microscope. Altered parts of the samples characterised by chromatic alteration were then subjected to X-ray diffraction analysis to detect mineral phases that could be related to the observed alteration form; the measurements were collected using a Bruker D2-Phaser diffractometer at the University of Pisa with the following measurements conditions: 5°- 65° 2θ, 0.02° 2θ step size, 2 s per step. Additionally, the red surfaces were investigated in more detail using micro-Raman spectroscopy and data were collected from polished cross sections and small sample chips, using Jobin-Yvon Horiba XploRA Plus apparatus equipped with 532 and 785 nm excitation sources and an Olympus BX41 microscope with 10, 50 and 100× objective lenses, at the University of Pisa. The minimum lateral and depth resolutions were set to a few μm. The system was calibrated using a 520.6 cm^{-1} Raman band of silicon before each experimental session. Spectra were collected through multiple acquisitions with counting times ranging from few seconds to two minutes. Backscattered radiation was analysed with a 1200 mm^{-1} grating monochromator. The characteristics of the dark deposits and chromatic alteration were examined using

micromorphological and chemical analysis at the stone surface; data were collected from carbon-coated sample chips by means of field emission scanning electron microscopy FEI Quanta 450 ESEM FEG equipped with a Bruker EDS QUANTAX XFlash detector, at the Centre for Instrument Sharing of the University of Pisa, (CISUP).

Geological samples were subjected to thermal aging to mimic the effect of high temperature stress on the stone (Franzoni et al. 2013; Ban et al. 2016) and to compare textural and compositional changes with those observed for the Pisa Cathedral samples. The cylinders were aged at the University of Pisa in a Nabertherm Gmbh furnace at 300 °C, 400 °C and 600 °C for 1h, with a temperature ramp of 6 °C/s, 4.5 °C/s and 3 °C/s, respectively. Cooling times were set to 3 °C/s, 2.5 °C/s and 1.5 °C/s, respectively. Capillary absorption tests were conducted on the geological samples according to the UNI EN 10859 (2000) standard recommendation, to evaluate possible physical changes due to thermal aging. Micromorphological and chemical analyses were carried out on carbon-coated polished sections of both fresh and aged samples using field emission scanning electron microscopy FEI Quanta 450 ESEM-FEG equipped with a Bruker EDS QUANTAX XFlash Detector, at CISUP, for comparative purposes.

Results

Cathedral samples

Stone alteration patterns

Chromatic alteration, dark deposits and salt crystallization in the open outermost porosity were the main alteration patterns observed with the light microscope on the stone sample surfaces. For the samples affected by chromatic alteration, the stone colour turns from yellow to red (*e.g.*, 1.d, 3.b, 3.c, 3.e) (Fig. 5.a) and a sharp boundary between altered and unaltered areas was observed (Fig. 5.b). The microstructure consists of elongated and angular grains and fossil fragments embedded in a calcite cement and a slight variability in the cement/grain ratio was observed among the studied samples (*e.g.*, a higher cement proportion in 3.b and 3.c). In the unaltered and yellow areas the bioclast fragments are clearly visible (*e.g.*, 2.a, 2.b) and the porosity is estimated at about 10-20% vol. In the red altered areas bioclast fragments are partially obliterated, and the porosity increases to 20-30% vol. The dark deposit is about 1 cm in thickness (*e.g.*, in 3.c and 3.d) and appears to be homogeneously distributed on the stone surface (Fig. 5.c). Under the deposit, the stone is altered and appears red. The presence of the dark deposits obliterates the textural features of the stone, and also fills the outermost porosity. In all samples, the open and outermost porosity is indicated by the presence of secondary crystalline phases (*e.g.*, in 1.d, 3.c, 3.d and 3.e), especially in darkening areas (Fig. 5.d).

Mineralogical-petrographic analysis

The stone is a biosparite (according to Folk 1959, 1962) or grainstone (according to Dunham 1962) (Fig. 6). Allochems (2 mm – 50 μm) are due to fragments of foraminifera, lamellibranchia, gasteropoda and algae (70% vol.). The orthochem fraction is due to spathic calcite (microsparite or pseudosparite), enriched by yellow iron oxides particles. A silicoclastic fraction (10-20%) due to quartz and plagioclase grains (3 mm - 300 μm) is present. Few intraclasts due to sandstone fragments and altered rock fragments (with chlorite/sericite) are also present. The porosity (25%-35% vol.) can be classified as interparticle, intraparticle and moldic (Choquette and Pray 1970). In the altered samples, a secondary porosity due to fractures and micro-fissures is observed and the

bioclast edges, cement and pores are characterised by a thick red concentration of fine-grained iron oxide/hydroxide minerals. No evident lithofacies variations were observed among the samples that were representative of the various analysed structures.

X-ray diffraction data collected from the altered and unaltered areas revealed the occurrence of (in order of abundance) calcite, quartz, albite, anorthite and biotite (Table 2). In some cases, small amounts of gypsum were identified. As expected, the bulk analysis did not enable us to detect and characterise the iron oxides, or to identify mineralogical differences between altered and unaltered areas. Unfortunately, due to the small amount of available samples from the Cathedral site, obtaining and characterising the insoluble stone residue through acid attack was not possible.

Micro-Raman analysis on red-altered areas

The micro-Raman data collected on the red altered areas enabled the identity of the iron oxide to be determined. The measurements identified the spectroscopic fingerprint of hematite, with typical Raman modes at 226, 292, 411 e 1320 cm^{-1} (de Faria et al. 1997), and an additional Raman broad band centred at 657 cm^{-1} was also visible (Fig. 7). According to de Faria and Lopes (2007) this Raman fingerprint is typical of crystalline disorder in heated goethite, forming hematite. When goethite is subject to heating, the Raman bands experience a shift towards a higher wavenumber of between 250 °C and 300 °C, and at above 260 °C the typical hematite Raman modes were identified at 224, 294, 408, 610, 657 e 1320 cm^{-1} along with an intense and broad band at 657 cm^{-1} (de Faria and Lopes 2007). Thus, the Raman spectroscopic features identified in the altered red areas suggest a mineralogical transformation of goethite into hematite due to heating at a range of 260-300 °C, with a consequent colour change of the stone from its original yellow-ochre colour to red.

Micro-morphological and chemical analysis on altered red surfaces and on dark deposits

Micro-morphological observations revealed particular features in the altered red areas, which are characterised by a collapse of the cement matrix microstructure (*i.e.*, an absence of the typical grain boundaries) and the presence of tiny and abundant iron oxides, scattered in the cement (Fig. 8.a). The dark deposits are characterised by a granular texture (Fig. 8.b), and the EDS chemical analysis revealed a composition corresponding to Ca-carbonate along with Si and low and variable amounts of Fe and Al. Traces of Cl, S, Mg and Na were also identified (Table 3). The most interesting result is represented by the detection of small Pb particles scattered in the dark deposits (Fig. 8.c-d). The EDS spectra and the analyses (Table 3) suggest an association of Pb with Cl (Pb-chloride minerals) and exclude the occurrence of Pb-sulphate (S is found in traces in the dark deposit but is not associated with Pb). Lead oxides and the metallic form of Pb, condensed after vaporisation due to the fire, cannot be excluded. However, the small size of these particles and the irregular surface prevented a quantitative analysis, so it is not possible to give a univocal interpretation. Pb particles are exclusively associated with the dark deposit.

Geological samples

The heating of the samples collected from geological outcrops induced chromatic alteration, and physical and textural changes at the stone. The rock turns a light red colour at 300 °C, red at 400 °C and light red at 600 °C (Fig. 9.a). A comparative evaluation of water behaviour between fresh and aged samples identified a slight

decrease of the capillary absorption coefficient up to 300 °C (from 1.08 g/cm^2∗√s in fresh samples to 0.81 g/cm^2∗√s), with a subsequent increase above 400 °C (1.22 g/cm^2∗√s). The capillary absorption coefficient quadrupled in samples subjected to 600 °C (4.23 g/cm^2∗√s) (Fig. 9.b-c). BSE images collected from the reference fresh sample identified the typical textural features of the rock, characterised by calcite (and dolomite), spathic cement (calcite crystal boundaries are clearly visible, along with dolomite crystals), fine-grained aggregates with variable amounts of Si, Al, Mg, K, Fe, Mn (possibly a clay proportion enriched by iron hydroxides, or iron-bearing clays) and, locally, Mn oxides (Fig. 10.a). Fe and Ti oxides are also scattered in the cement, possibly related to the intraclasts observed in thin section. Interesting textural and compositional changes were observed in the sample heated at 300 °C. The cement texture is partially obliterated and crystal boundaries are no longer visible (Fig. 10.b). The inter-crystalline sites and the inner porosity of the bioclasts (bioclast porosity) are characterised by tiny and abundant iron oxides. In the sample heated to 400 °C a collapse of the cement structure was observed (the cement crystal boundaries can no longer be recognised); the iron oxide crystal areas have increased and micro-cracks have developed (Fig. 10.c-d). In the sample heated to 600 °C the textural features are completely obliterated, the iron oxide areas have increased, newly formed iron oxides partially fill the bioclast porosity (Fig. 10.e) and intense microfracture systems have developed (Fig. 10.f).

Discussion

The thermal aging of the geological samples enabled us to evaluate the effects of thermal stress on the Panchina Fm. calcarenite lithotype, and its behaviour is in accordance with the literature (Yavuz et al. 2010). The stone turns in fact from yellow to red when heated to between 300 °C and 400 °C. The lithotype exhibits a reduction of porosity (and thus of capillary absorption) when heated at temperatures up to 300 °C, due to textural changes into the cement structure (i.e., its collapse), as observed in the SEM-BSE images. As Bebck et al. (2016), Hajpal and Torok (2004), Martinho and Dionisio (2020) found for similar lithotypes, when heated to between 300 °C and 400 °C the stone experiences a porosity increase and a growth of iron oxide areas (particularly evident up to 400-600 °C), as the SEM observations reveal. Finally, at 600 °C the stone is affected by an intense microfracture system, with a consequent porosity increase; the changes in texture and structure identified by the SEM investigations support the measured quadruple capillary absorption values.

The physical, micro-morphological and chemical analyses conducted on the altered specimens taken from the Cathedral and the comparison with heated geological samples enabled us to plausibly interpret the observed patterns in the Cathedral stones as the effects of exposure to high temperatures and thus to the effects of a fire. The altered red samples exhibit a colour hue similar to the aged sample heated at 300-400 °C, and the textural features are comparable with those developed in the aged sample heated to 400 °C, *i.e.,* obliterated cement grain boundaries and increased iron oxide areas. The Raman analysis conducted on the red altered areas revealed the typical fingerprint of heated goethite, likely transformed at around 300 °C into hematite. Finally, we can identify a correlation between the observed fire-induced alteration patterns and the effects of the fire that affected Pisa Cathedral in 1595. The analysis of the dark deposits supports this hypothesis due to the detection of significant amounts of lead particles. According to historical sources (Casini 1986), the fire was responsible for the complete melting of the original lead covering the structures of the Cathedral, similar to the recent disaster in Notre-Dame de Paris (Ferreira 2019; Le Roux et al., 2019).

Lead particles on dark deposits were also detected on the altered samples taken from the flying buttresses, inside the gap generated by the structural separation. Thus, the traces of fire appear to offer a *terminus ante quem* in dating the crack pattern of the east and west flying buttress, namely that the cracks had already formed when the fire occurred in the Cathedral.

Further insights into the origin of this crack pattern are provided by the on-going archaeological study of the brick masonry infill "β" (Fig. 1.c), which probably dates back to the late Middle Ages. As the masonry infill is not damaged nor detached from the adjacent structures and is affected by chromatic alteration, it was likely to have been built after the formation of the cracks on the flying buttress and before the fire of 1595. The crack patterns were thus probably produced many centuries before the 1595 fire by soil consolidation and related to the renowned leaning phenomenon of Pisa Tower. The cause of this will be assessed in the on-going structural analysis.

Conclusions

Monuments represent our historic heritage, and our duty is to preserve them for future generations. The protection of historical building assets is achieved through acquiring detailed knowledge from history about the phases of construction, and by characterising the constituent materials and assessing their state and conservation. Examining the construction materials can inform the reconstruction of the events that ancient buildings have experienced and can also reveal new details about specific occurrences or the present conservation state.

This study provides a mineralogical and petrographic characterisation of the calcarenite Panchina Fm. lithotype used in the masonry of Pisa Cathedral and a description of its thermal behaviour, revealing the main chromatic, mineralogical and physical changes through the application of high temperatures. The analysis of the calcarenite samples from the *matroneum* demonstrates that all of the investigated structures were involved in the fire that occurred in 1595.

The fire appears to have only affected the stone masonry surface, and chromatic alterations and micro-cracks were observed in a centimetric layer below the stone surface, on which dark deposits containing lead particles were also identified, which are interpreted as due to the melting of the roof structures.

The fire was not responsible for the existing structural damage, which can be related to other geological causes still under investigation, but its effects on calcarenite stone can help to date the origins of the structural damage to the flying buttress, and therefore also the cracks on the intrados of the arch supporting the dome.

The damage assessment of Pisa Cathedral shows once again that the diagnostic process for cultural heritage structures requires a multi- disciplinary and dynamic approach that involves different types of information. Detailed knowledge of the specific materials of the Cathedral is essential in investigations into its structural damage, and will be key to reconstructing the chain of events that generated the detected crack pattern.

Acknowledgments

The authors acknowledge the Opera Primaziale Pisana (OPAE Pisa) for supporting this study, and enabling access to the worksite and the sampling of the stone specimens. Thanks to R.I and D.M. for technical assistance during the analysis. S.R. acknowledges the financial support of PRA-2018-41 project (Georisorse e Ambiente) funded by the University of Pisa. We thank two anonymous reviewers for their constructive comments.

References

Alberti A, Parodi L, Mitchell J (2011) La Cattedrale prima di Buscheto (Periodo IV). In: Alberti A. and Paribeni E (ed) Archeologia in Piazza dei Miracoli: Gli scavi 2003-2009, Felici Editore, Pisa, pp 243-267.

Andriani GF, Germinario L (2014) Thermal decay of carbonate dimension stones: fabric, physical and mechanical changes. Environmental Earth Sciences 72:2521-2539. https://doi.org/10.1007/s12665-014-3160-6

Ascani V (2014) Il Duomo di Pisa. Architettura e scultura architettonica dalla fondazione al Quattrocento. In: Garzella G, Caleca A, Collareta M (eds) La Cattedrale di Pisa, Pacini Editore, Pisa, pp 84-110.

Ban M, Baragona AJ, Ghaffari E, Weber J, Rohatsch A (2016) Artificial aging techniques on various lithotypes for testing of stone consolidants. In: Hughes J, Howind T (eds) Science and Art: A Future for Stone: Proceeding of the 13th International Congress on the Deterioration and Conservation of Stone, Volume 1. Paisley, pp 253-260.

Beck K, Janvier-Badosa S, Brunetaud X, Torok A, Al-Mukhtar M (2016) Non-destructive diagnosis by colorimetry of building stone subjected to high temperatures. European Journal of Environmental and Civil Engineering 20:643-655. https://doi.org/10.1080/19648189.2015.1035804

Bennati S, Aita D, Barsotti R, Caroti G, Chellini G, Piemonte A, Barsi F, Traverso C (2020) Survey, experimental tests and mechanical modeling of the dome of Pisa Cathedral: a multidisciplinary study. International Journal of Masonry Research and Innovation 5:1. https://doi.org/10.1504/IJMRI.2020.104850

Borg RP, Hajpal M, Torok A (2013) The fire performance of limestone characterization. Characterizion strategy for the fire performance of Maltese & Hungarian limestone. In: Wald F. (ed) International conference proceedings, Application of Structural Fire Engineering. Prague.

Brotons V, Tomas R, Ivorra S, Alarcon JC (2013) Temperature influence on the physical and mechanical properties of a porous rock: San Julian's calcarenite. Engineering Geology 167:117-127. https://doi.org/10.1016/j.enggeo.2013.10.012

Casini C (1986) I restauri seicenteschi del Duomo di Pisa. Bollettino storico pisano LV:149-170.

Choquette PW and Pray LC (1970) Geologic Nomenclature and Classification of Porosity in Sedimentary Carbonates. American Association of Petroleum Geologists Bulletin 54:207-250.

De Faria DL and Lopes FN (2007) - Heated goethite and natural hematite: Can Raman spectroscopy be used to differentiate them?. Vibrational Spectroscopy 45:117-121. https://doi.org/10.1016/j.vibspec.2007.07.003

De Faria DL, Venâncio Silva S, De Oliveira MT (1997) Raman microspectroscopy of some iron oxides and oxyhydroxides. Journal of Raman Spectroscopy 28:873-878. https://doi.org/10.1002/(SICI)1097-4555(199711)28:11<873:AID-JRS177>3.0.CO;2-B

Dunham RJ (1962) Classification of carbonate rocks according to depositional texture. In: Ham W.E. (ed) Classification of carbonate rocks – a symposium. American Association of Petroleum Geologists, Tulsa, pp 108-121.

Ferreira TM (2019) Notre Dame Cathedral: Another Case in a Growing List of Heritage Landmarks Destroyed by Fire. Fire, 20. https://doi.org/10.3390/fire2020020

Folk RL (1962) Spectral subdivision of limestone types. In: Ham WE (ed) Classification of Carbonates Rocks – a symposium. American Association of Petroleum Geologist, Tulsa, pp. 62-84.

Folk RL (1959) Practical petrographic characterization of limestones. American Association Petroleum Geologist Bulletin 43:1-38.

Franzini M (1993) Le pietre toscane nell'edilizia medioevale della città di Pisa. Memorie Società Geologica Italiana II:233-244.

Franzoni E, Sassoni E, Scherer GW, Naidu S (2013) Artificial weathering of stone by heating. Journal of Cultural Heritage 14:85-93. https://doi.org/10.1016/j.culher.2012.11.026

Galai H, Nahdi K, Trabelsi-Ayadi M (2007) Study of isothermal behavior of natural Tunisian dolomite under controlled pressure of carbon dioxide. Asian Journal of Chemistry 19: 4231-4244.

Galoppini R, Mazzanti R, Tessari R, Taddei M, Viresini L (1996) Le cave di arenaria lungo il litorale livornese. Quaderni del Museo di Storia Naturale di Livorno 14:111-146.

Gomez-Heras M, Fort R, Morcillo M, Molpeceres C, Ocana L (2008) Laser heating: A minimally invasive technique for studying fire-generated heating in building stone. Materiales de Construccion 58:289-290. https://doi.org/10.3989/mc.2008.v58.i289-290.82

Gunasekaran S and Anbalagan G (2007) Thermal decomposition of natural dolomite. Bull. Mater. Sci. 30: 339-344. https://doi.org/10.1007/s12034-007-0056-z

Hajpal M (2002) – Changes in sandstones of historical monuments exposed to fire or high temperature. Fire Technology 38: 373-382. https://doi.org/10.1023/A:1020174500861

Hajpal M and Torok A (2004) Mineralogical and colour changes of quartz sandstones by heat. Environmental Geology 46:311-322. https://doi.org/10.1007/s00254-004-1034-z

International Scientific Committee for Stone (ISCS) (2008) Illustrated glossary on stone deterioration patterns. ICOMOS, France.

Jansen DP, Carlson SR, Young RP, Hutchins DA (1993) Ultrasonic-imaging and acoustic-emission monitoring of thermally-induced microcracks in Lac-du-Bonnet-granite. Journal of Geophysical Research-Solid Earth 98:22231-22243. https://doi.org/10.1029/93JB01816

Kilic O and Anil M (2006) Effect of limestone characteristic properties and calcination temperature on lime quality. Asian Journal of Chemical 18: 655-666

Kompanikova Z, Gomez-Heras M, Michnova J, Durmekova T, Vicko J (2014) Sandstone alterations triggered by fire-related temperatures. Environmental Earth Sciences 72:2569-2581. https://doi.org/10.1007/s12665-014-3164-2

Le Roux G, De Vleeschouwer F, Weiss D, Masson O, Pinelli E, Shotyk W (2019) Learning from the Past: Fires, Architecture, and Environmental Lead Emissions. Environmental Science & Technology 53: 8482-8484. https://doi.org//10.1021/acs.est.9b03869.

Martinho E and Dionísio A (2020) Assessment Techniques for Studying the Effects of Fire on Stone Materials: A Literature Review. International Journal of Architectural Heritage 14:275-299. https://doi.org/10.1080/15583058.2018.1535008

McCabe S, Smith BJ, Warke PA (2007a) Sandstone response to salt weathering following simulated fire damage: A comparison of the effects of furnace heating and fire. Earth Surface Processes and Landforms 32:1874-1883. https://doi.org/10.1002/esp.1503

McCabe S, Smith BJ, Warke PA (2007b) Preliminary observations on the impact of complex stress histories on the response of sandstone to salt weathering: Laboratory simulations of process combinations. Environmental Geology 52:269-276. https://doi.org/10.1007/s00254-006-0531-7

McCabe S, Smith BJ, Warke PA (2010) Exploitation of inherited weakness in fire-damaged building sandstone: The "fatiguing" of "shocked" stone. Engineering Geology 115:217-225. https://doi.org/10.1016/j.enggeo.2009.06.003

Montevecchi N, Sutter A (2014) Il restauro dell'abside del Duomo di Pisa: un cantiere per la conoscenza e la conservazione. In: Garzella G, Caleca A, Collareta M (eds) La Cattedrale di Pisa, Pacini Editore, Pisa, pp 259-267.

Munsell Color (Firm). (2010). Munsell soil-color charts: With genuine Munsell color chips. Grand Rapids, MI: Munsell Color.

Ozguven A and Ozcelik Y (2013) Investigation of some property changes of natural building stones exposed to fire and high heat. Construction and Building Materials 38:813-821. https://doi.org/10.1016/j.conbuildmat.2012.09.072

Pires V, Rosa LG, Dionisio A (2014) Implications of exposure to high temperatures for stone cladding requirements of three Portuguese granites regarding the use of dowel-hole anchoring systems. Construction and Building Materials 64:400-450. https://doi.org/10.1016/j.conbuildmat.2014.03.035

Ramacciotti M, Spampinato M, Lezzerini M (2015) The building stones of the apsidal walls of the Pisa's Cathedral, Atti Società Toscana di Scienze Naturali, Memorie, Serie A 122:55-62.

Sanpaolesi P (1970) Il Duomo di Pisa: rilievo a cura dell'Istituto di restauro dei monumenti. Nistri-Lischi, Pisa.

Sarti G, Bertoni D, Capitani M, Ciampalini A, Ciulli L, Cerrina Feroni A, Andreucci S, Zanchetta G (2017) Facies analysis of four superimposed trasgressive-regressive sequences formed during the two-last interglacial-glacial cycles (Central Tuscany, Italy). Atti Società Toscana di Scienze Naturali, Memorie, Serie A, 124: 133-150. http://dx.doi.org/10.2424/ASTSN.M.2017.24

Sippel J, Siegesmund S, Weiss T, Nitrsch H, Korzen M (2007) Decay of natural stones cause by fire. Geological Society, London.

UNI EN 10859 (2000) Beni Culturali. Materiali Lapidei naturali ed artificiali. Determinazione dell'assorbimento d'acqua per capillarità. UNI, Ente Nazionale Italiano di Unificazione, Milano.

Vazquez P, Acuna M, Benavente D, Gibeaux S, Navarro I, Gomez-Heras M (2016) Evolution of surface properties of ornamental granitoids exposed to high temperatures. Construction and Building Materials 104:263-275. https://doi.org/10.1016/j.conbuildmat.2015.12.051

Watt DS (1999) Building patholgy: principles and practice. Blackwell, Oxford.

Woodcock DG (1997) Reading buildings instead of books: historic structure reports as learning tools. APT Bulletin 28:37-38.

Yavuz H, Demirdag S, Caran S (2010) Thermal effect on the physical properties of carbonate rocks. International Journal of Rock Mechanics and Mining Sciences 47:94-103. https://doi.org/10.1016/j.ijrmms.2009.09.014

Figure and Table captions

Figure 1. (a) The Cathedral and the Miracle Square complex. (b) Schematic view of the rear façade (Sanpaolesi 1970); on both north and south sides, flying buttresses connect the arch to the external walls of the transepts. Details of the (c) east and (d) west arches and flying buttress affected by the crack pattern.

Figure 2. Localisation of stone specimens sampled at the Pisa Cathedral's *matroneum*. Modified from Sanpaolesi (1970).

Figure 3. (a) Internal surface of the wall facing the choir - under the blind arcade - affected by red chromatic alteration (area A). (b-c) Stone ashlar of the flying buttress adjacent the east arch affected by cracks and dark deposits on the stone surface (area A). (d-e) Surface of the wall facing the main nave (area C).

Figure 4. Details of the masonry infill "α", area B.

Figure 5. Macro-pictures of studied samples demonstrating the observed alteration patterns: (a) chromatic alteration (sample 1.d); (b) sharp interface between altered and unaltered areas (sample 1.d); (c) dark deposit (sample 3.c) and (d) salt crystallisation into outermost porosity (sample 3.c).

Figure 6. Microphotographs of the examined stone with indications of the main textural and structural features. All: allochems; Sp: sparite; Inter_v: inter-particle voids; Intra_v: intra particle voids. Samples (a) 2.b and (b) 4.b, are shown as examples.

Figure 7. Raman spectrum collected on a reddish altered area in 3.e reddened sample, as an example.

Figure 8. BSE images collected on altered areas. (a) Surface affected by chromatic alteration. (b) Dark deposits due to granular aggregates showing the presence of Pb particles (c-d).

Figure 9. Stone samples subjected to thermal aging and physical properties. (a) (from left to right) fresh stone, stone heated to 300°C, 400°C and 600°C. (b) Water absorption by capillarity before and after thermal aging. (c) Capillary absorption coefficient calculated for fresh and aged samples.

Figure 10. BSE images collected on fresh natural sample (a) and thermal altered samples at (b) 300°C, (c-d) 400°C and (e-f) 600°C.

Table 1. List of examined samples and brief descriptions of observed alteration forms. M.I. = Munsell Index (Munsell, 2010).

Table 2. Semi-quantitative mineralogical composition of the bulk rock. Cc = calcite; Qtz = quartz; Fsp = feldspars; Bt = biotite; Gp = gypsum. xx = abundant; x = scarce; tr = traces; – = absent.

Table 3. Semi-quantitative chemical composition of the dark deposit (analysis n. 1-4, raster windows approx. 80x80 square microns) and of the Pb-rich particles identified on the dark coatings (analysis n. 5-8). Bdl: below detection limit.

Table 1. List of studies samples and brief description of observed alteration forms. M.I. = Munsell Index (Munsell, 2010)

Sample site	Sampling area	Sample ID	Description
Pisa Cathedral	Area A: wall facing the choir, under the blind arcade	3a-b	chromatic alteration; stone surface turns from yellow/reddish-yellow (M.I 7.5YR 7/6-7/8) to red (M.I 2.5YR 5/6) sharp boundary between altered and unaltered areas
	Area A: flying buttress adjacent the East arch supporting the dome	3c	chromatic alteration; stone surface turns from yellow/reddish-yellow (M.I 7.5YR 7/6-6/8) to red (M.I 2.5YR 5/6). Sharp boundary between altered and unaltered areas
	Area A: wall facing the choir, under the blind arcade	3d	dark deposit (M.I 5YR 2.5/2, dark reddish brown) about 1 cm in thickness under the deposit, the stone is altered and colour turns in red (M.I 5YR 5/6)
	Area B: masonry infill "α"	1a-g	chromatic alteration; stone surface turns from yellow (M.I 7.5YR 7/6) to red, light red (M.I 2.5YR 5/6-6/6) sharp boundary between altered and unaltered areas
	Area B: masonry infill "α"	2a-b	No alteration patterns or decay forms. Stone surface is yellow (M.I 7.5YR 6/8)
	Area C: flying buttress adjacent to the West arch supporting the dome	4a-b	dark deposit (M.I 7.5YR 4/2-4/3, brown) about 1 cm in thickness under the deposit. In 4a the stone is brownish yellow (7.5 YR 6/8). In 4b the stone is altered and colour turns in red (M.I. 2.5YR 5/6)
	Ares C: inner surface of the wall facing the main nave	4c-e	chromatic alteration; stone surface is red (M.I. 2.5YR 5/6)
Outcrops Panchina	Castiglioncello (Livorno, Italy)	Fresh sample	Coarse grained calcarenite, yellow in colour (7.5YR 7/6) with bioclasts

Fm. calcarenite			and detrital fractions
		Heated 300 °C	chromatic alteration; stone surface turns from yellow (M.I 7.5YR 7/6) to light red (M.I 2.5YR 6/6)
		Heated 400 °C	chromatic alteration; stone surface turns from yellow (M.I 7.5YR 7/6) to red (M.I 2.5YR 5/6)
		Hetaed 600 °C	chromatic alteration; stone surface turns from yellow (M.I 7.5YR 7/6) to light red (M.I 2.5YR 7/6)

Table 2. Semi-quantitative mineralogical composition of the bulk rock. Cc = calcite; Qtz = quartz; Fsp = feldspars; Bt = biotite; Gp = gypsum. xx = abundant; x = scarce; tr = traces; – = absent.

	Sample ID	Qtz	Cc	Fsp	Bt	Gp
Bulk rock, not altered area	1d	x	xxx	x		
Bulk rock, chromatic alteration	1d	x	xxx	x		
Bulk rock, chromatic alteration	3d	x	xxx	x		
Bulk rock, chromatic alteration	4c	x	xxx	x	tr	tr

Table 3. Semi-quantitative chemical composition of the dark deposit (analysis n. 1-4, raster windows approx. 80x80 square microns) and of the Pb-rich particles identified on the dark coatings (analysis n. 5-8). Bdl: below detection limit.

sample	**3c**	**3c**	**3c**	**3d**	**3d**	**3d**	**3d**	**3d**
analysis n.	1	2	3	4	5	6	7	8
type	area	area	area	area	spot	spot	spot	spot
Na_2O wt%	0.96	0.52	0.79	bdl	bdl	1.06	0.55	0.31
MgO	2.31	bdl	0.55	2.34	bdl	bdl	0.43	bdl
Al_2O_3	2.70	0.59	0.55	0.86	bdl	0.28	0.27	bdl
SiO_2	55.25	52.39	37.22	1.43	0.36	0.80	1.17	0.75
SO_3	1.72	9.79	9.38	3.51	bdl	bdl	bdl	bdl
K_2O	0.99	bdl	0.27	0.00	1.62	1.41	bdl	bdl
CaO	30.24	36.24	50.15	91.85	6.05	8.37	15.66	7.42
FeO	5.84	bdl	bdl	0.00	bdl	bdl	bdl	bdl
MnO	bdl	bdl	bdl	0.00	bdl	bdl	bdl	bdl
PbO	bdl	bdl	bdl	0.00	70.89	71.20	70.79	88.31
P_2O_5	bdl	bdl	0.60	0.00	0.10	bdl	7.66	bdl
Cl	bdl	0.47	0.48	0.00	20.99	16.88	3.48	3.21
sum	100.00	100.00	100.00	100.00	100.00	100.00	100.00	100.00